Catalysis Letters 53 (1998) 37–42

Microstructure of a Pd/ceria–zirconia catalyst after high-temperature aging

J.C. Jiang [a], X.Q. Pan [a,*], G.W. Graham [b], R.W. McCabe [b] and J. Schwank [c]

[a] *Department of Materials Science and Engineering, The University of Michigan, Ann Arbor, MI 48109, USA*
E-mail: panx@umich.edu
[b] *Chemical and Physical Sciences Laboratory, Ford Motor Company, MD3179/SRL, PO Box 2053, Dearborn, MI 48121, USA*
[c] *Department of Chemical Engineering, The University of Michigan, Ann Arbor, MI 48109, USA*

Received 27 February 1998; accepted 29 April 1998

A model automotive exhaust catalyst, consisting of 2.25 wt% Pd supported on initially high-surface-area (88 m^2/g) cerium–zirconium mixed oxide ($Ce_{0.5}Zr_{0.5}O_2$), was studied by X-ray diffraction (XRD), thermogravimetric analysis (TGA), and transmission electron microscopy (TEM), following high-temperature (1150 °C) redox aging. Spherical Pd particles with size varying from 30 to 80 nm in diameter were found to be embedded both within single grains and at interfaces between multiple grains of the mixed oxide. X-ray energy-dispersive spectroscopy (EDS) and microbeam electron diffraction show that these particles are pure Pd, with face-centered-cubic structure. These results, together with elemental distribution maps obtained by EDS imaging, provide detailed visualization of an encapsulation phenomenon previously reported on the basis of XRD and TGA measurements alone.

Keywords: particle encapsulation, Pd catalyst, cerium–zirconium mixed oxide, electron microscopy, TEM

1. Introduction

Automotive exhaust catalysts have to function for long periods of time under harsh conditions, especially in terms of temperature. While earlier generations of automotive catalysts had an operational limit of about 750 °C, improved catalyst formulations have extended the range up to 950 °C. Current practice is to limit the catalyst temperature by operating the engine in an excessively fuel-rich regime to avoid thermal degradation of the catalyst. However, to achieve optimum fuel economy when automotive engines operate under high speed or load conditions, the catalytic converter temperatures would have to be as high as 1050 or even 1100 °C. This would lead to lower consumption of fuel and, as an added benefit, lower levels of exhaust emissions. A prerequisite for developing such thermally stable catalysts is a good understanding of the thermal deactivation modes contributing to the aging and degradation of catalysts in harsh thermal environments. Much of the improvement in thermal stability of automotive catalysts in recent years has come from the use of micron-sized particles of ceria–zirconia solid solutions both for supporting the active noble metals and serving as oxygen storage agents. Although these materials undergo tremendous loss of surface area after aging at the temperatures indicated above, they are superior to ceria–zirconia (or pure ceria) supported along with the noble metals on more refractory oxides such as alumina. The reasons for this are that: (1) composition of the solid solutions can be precisely controlled and optimized for best oxygen storage characteristics, (2) contact between the noble metals and the ceria–zirconia is assured no matter how extensively the materials sinter, and (3) rates of bulk oxygen transport are sufficient to ensure high rates of oxygen storage and release even in the absence of high surface area [1]. Given the wide utilization of these ceria–zirconia materials, a model automotive exhaust catalyst consisting of Pd supported on initially high-surface-area ceria–zirconia is examined, in the present study, after high-temperature aging in order to follow up on an earlier discovery that upon such aging, Pd sinters into large (tens of nanometers in diameter) particles, some of which seemed to be encapsulated within the ceria–zirconia [2]. Interestingly, the X-ray diffraction (XRD) patterns of these Pd particles gave evidence for significant (about 3 vol%) compression of the Pd lattice, creating a high residual stress in the metal particles. The authors accounted for this stress by proposing the following scenario: Pd, which remains zero-valent, even in the presence of 0.5 mol% O_2 at 1050 °C, sinters into large particles, several tens of nanometers in diameter. The ceria–zirconia matrix also sinters, but alternately expands and contracts under the reducing and oxidizing portions of the aging treatment due to the difference in size between Ce^{3+} and Ce^{4+}. During these events, some of the Pd particles become encapsulated within the mixed oxide while it is in a partially reduced state. Ultimately, however, the mixed oxide is left in its fully oxidized state, thus creating the residual stress (as high as 3.6 GPa).

There are many important issues to be resolved with regard to the thermal degradation in this case. For example, it would be important to find out whether the metal particles start to sinter before the pore volume of the mixed-

* To whom correspondence should be addressed.

oxide support starts to shrink. Another open question is whether or not the metal particles are "squeezed" out of the oxide as the pore structure starts to collapse. It is also important to know why some of the metal particles become encapsulated by the support whereas others do not. To begin to address these questions, a combination of transmission electron microscopy (TEM) images, elemental maps obtained by X-ray energy-dispersive spectroscopy (EDS), and a microbeam electron diffraction pattern are presented together with complementary results from XRD and thermogravimetric analysis (TGA) to characterize and compare the ceria–zirconia-supported Pd catalyst after redox aging at temperatures of 1050 and 1150 °C.

2. Experimental details

The ceria–zirconia-supported Pd catalyst in this study is the same one as used previously [2]. This catalyst consists of 2.25 wt% Pd on $Ce_{0.5}Zr_{0.5}O_2$ with a specific surface area (BET) of 88 m^2/g after calcination at 600 °C for 12 h. Aging was performed by heating for 12 h in a flowing gas mixture containing 1 mol% CO/H_2 ($[CO]/[H_2] = 3/1$) alternating every 10 min with 0.5 mol% O_2; the remainder of the mixture consisted of 0.002 mol% SO_2, 10 mol% H_2O, and balance N_2. The maximum aging temperature for this study was 1150 °C, whereas previously it was 1050 °C [2]. After aging, samples were calcined for 2 h at 700 °C in order to convert all unencapsulated Pd to PdO. Specific surface area and XRD patterns were obtained as before [2]; TGA results were obtained in flowing air with a Perkin-Elmer TGA7 analyzer.

For TEM investigations, a large-size aggregate with diameter about 1 mm was selected from the aged catalyst powder, sandwiched between two supported silicon crystals, and cut into cross-sectional slices. The cross-sectional slices were glued on Cu rings and then thinned by mechanical grinding, polishing and dimpling, followed by low-angle Ar-ion milling to perforation. TEM studies were conducted within a JEOL 2000FX analytical electron microscope (AEM) equipped with an X-ray energy-dispersive spectrometer and parallel electron energy-loss spectrometer, operating at 200 kV.

3. Results

The XRD pattern of the catalyst after aging at 1150 °C was not much different than after aging at 1050 °C [2], except that the mixed-oxide peaks were about half the width, and there was a small (less than 10%) amount of tetragonal zirconia apparent in addition to the main mixed-oxide phase. The specific surface area after 1150 °C was less than 1 m^2/g (though non-zero), compared with 2.8 m^2/g after 1050 °C.

The (111) Pd peaks, due to Pd particles which formed in the process of aging at either 1050 or 1150 °C, are shown in figure 1(a) together with that of the reduced catalyst (subsequent to 1050 °C aging). The previous work suggested that these Pd particles are encapsulated in the mixed-oxide matrix due to the aging since they resist subsequent oxidation. (The PdO peak nearest to the (111) Pd peak appears at 41.9°, which is not within the domain of figure 1.) Compared with 1050 °C aging, the peak after 1150 °C aging is more intense, broader, and at smaller angle, indicating, respectively, that more Pd is encapsulated under a distribution of stress states, the average of which is lower. The intensity of both peaks may be compared with that of the reduced catalyst, in which stress applied to the encapsulated Pd particles by the ceria–zirconia mixed oxide has been relaxed:

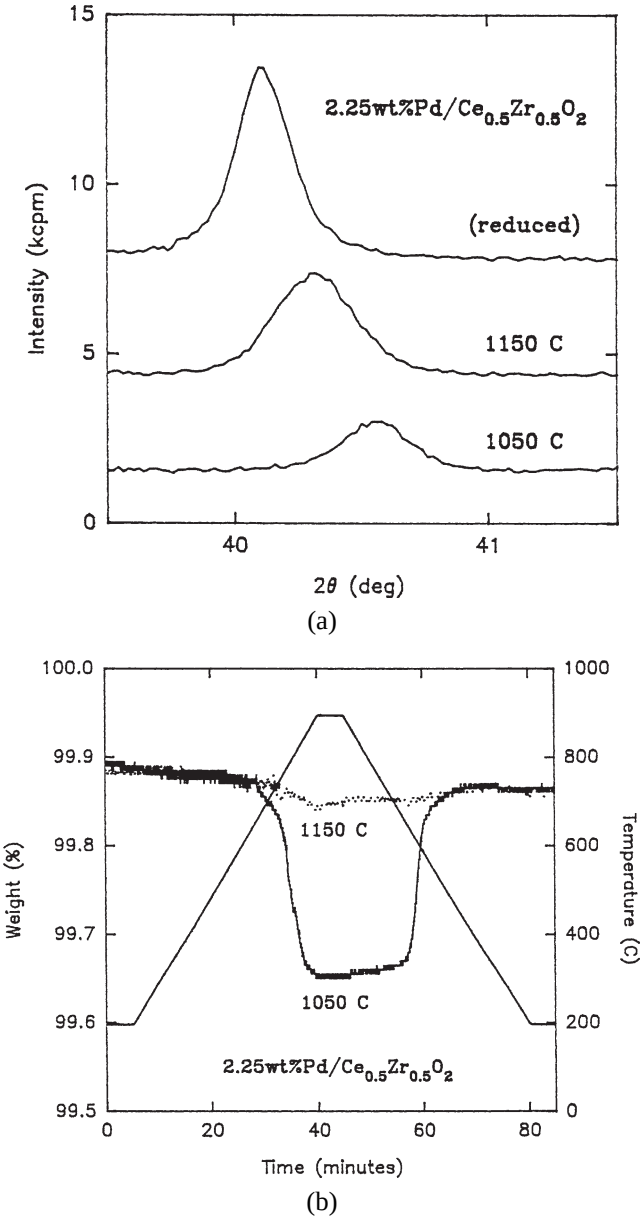

Figure 1. (a) XRD patterns showing the Pd(111) reflection from the catalysts aged at 1050 and 1150 °C (followed by oxidation at 700 °C) as well as the catalyst (aged at 1050 °C) following reduction. (b) Results from TGA measurements (performed by heating between 200 and 900 °C, as indicated, in air) of the catalysts after aging at 1050 and 1150 °C.

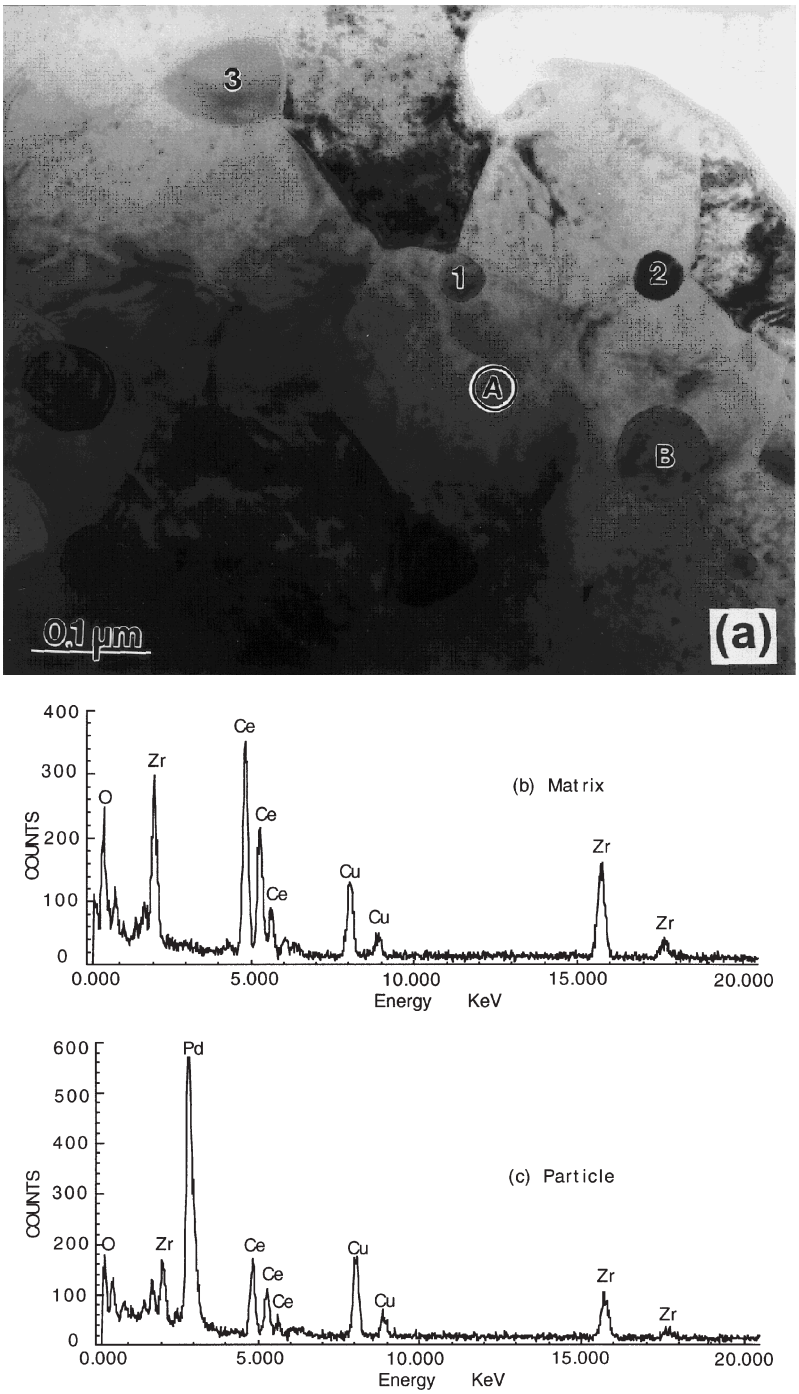

Figure 2. (a) Bright-field TEM micrograph showing Pd particles (B, 1, 2, and 3) embedded within the ceria–zirconia mixed oxide. (b) EDS spectrum from the ceria–zirconia mixed-oxide matrix (region A in (a)). (c) EDS spectrum from a Pd particle (region B in (a)).

the intensity after 1150 °C aging is roughly 85% of that of the reduced catalyst, whereas it is 25–30% of that of the reduced catalyst after 1050 °C aging.

These values may be compared with the TGA results shown in figure 1(b). Upon heating, PdO undergoes complete decomposition to Pd and O_2 by 900 °C in air. Although the expected weight loss due to decomposition of PdO in an oxidized catalyst containing 2.25 wt% Pd is 0.34%, the observed weight loss is only about 0.05% after 1150 °C, corresponding to a loss (through encapsulation) of 85% of the Pd, and about 0.24% after 1050 °C, corresponding to a loss of 29% of the Pd. The XRD and TGA measurements are thus in agreement regarding the extent of Pd encapsulation. With 85% of the Pd encapsulated after 1150 °C aging, this case presents a rather favorable situation for TEM investigations.

In order to reveal the detailed microstructure of the Pd catalysts after aging, studies were conducted using different TEM techniques including diffraction contrast images, microbeam electron diffraction, and EDS analysis. Figure 2(a)

Figure 3. (a) TEM micrograph using scanning TEM mode. (b)–(e) Element maps obtained by EDS of Pd, Zr, Ce, and O, respectively.

is a bright-field micrograph showing the typical microstructure of the catalyst after 1150 °C aging. The matrix material in figure 2(a) is identified to be the ceria–zirconia grains. In addition, there are small particles visible in figure 2(a). These particles are either embedded within single ceria–zirconia grains or surrounded by multiple ceria–zirconia grains. Since these particles always appear as round disks in TEM images, they should have a spherical shape. The size of these particles in figure 2(a) varies from 30 to 80 nm in diameter. In order to get a statistically significant size distribution of particles, many specimens were prepared and investigated by TEM. The average size of the particles is about 60 nm in diameter, based on the examination of numerous micrographs taken from different specimens.

The composition of particles in the specimen was determined by EDS analysis. Figure 2(b) is an EDS spectrum taken from the ceria–zirconia matrix, such as the region marked by letter A in figure 2(a). This spectrum shows the presence of Zr, Ce, and O. No Pd was detected in the matrix. (The occurrence of the Cu peaks in the spectrum is ascribed to scattering from the Cu ring.) Figure 2(c) is an EDS spectrum from a particle, such as the one marked by letter B in figure 2(a). It shows one intense Pd peak and other weak peaks resulting from Zr, Ce, O, and Cu. The Zr, Ce, and O peaks are presumed to be from the surrounding $Ce_{0.5}Zr_{0.5}O_2$ matrix, and the Cu peaks result from the Cu rings, as mentioned previously.

The spatial distribution of different phases existing in the specimen was also investigated by elemental maps using EDS imaging (figure 3). Figure 3(a) shows a micrograph obtained in the scanning TEM mode. It shows the same characteristic microstructure as in figure 2(a). The isolated dark regions in figure 3(a) correspond to the Pd particles. The spatial distribution of Pd, Zr, Ce, and O in this region is shown in the elemental maps in figure 3 (b)–(e), respectively. The regions with high intensity in figure 3(b) indicate highly Pd-rich areas. The bright regions in figure 3(b) have one-to-one correspondence to the dark regions in figure 3(a). The Zr, Ce, and O maps in figure 3 (c)–(e) show almost homogeneous contrast, except for some regions with slightly less intensity, corresponding to the positions of the highly Pd-concentrated particles. The reason for the very low contrast of these particles in the O, Zr, and Ce maps is that the size of the particles is small relative to the thickness of the specimen, which results in a large overlap between the particles and the matrix.

In order to further confirm that the particles observed are pure Pd (rather than an oxide or some other phase containing Pd), microbeam electron diffraction analysis was conducted. The microbeam electron diffraction patterns (figure 4) taken from the particles show that they have a face-centered-cubic structure with a lattice parameter of $a \approx 4.0$ Å, which corresponds to the crystallographic structure of pure Pd (face-centered-cubic structure with

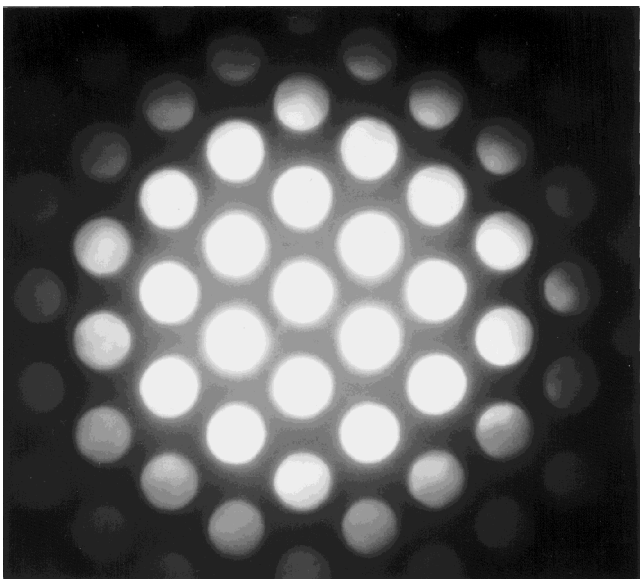

Figure 4. Micro electron diffraction pattern, taken from an embedded Pd particle, which corresponds to the [110] zone for electron diffraction from the face-centered-cubic structure of Pd.

$a = 3.8898$ Å) [3] (rather than PdO, for example, which is a tetragonal structure with $a = 3.043$ Å and $b = 5.337$ Å [4]).

4. Discussion

These studies have clearly demonstrated the existence of pure Pd particles in the aged catalyst. Both conventional and analytical TEM studies reveal that the particles observed are Pd metal (rather than Pd oxide) and have a spherical shape. These Pd particles are randomly distributed in the cerium–zirconium mixed-oxide matrix (figure 2(a)). They are embedded within either a single $Ce_{0.5}Zr_{0.5}O_2$ grain or between several $Ce_{0.5}Zr_{0.5}O_2$ grains. For example, particle 1 in figure 2(a) is embedded within one single grain whereas particle 2 is held between two $Ce_{0.5}Zr_{0.5}O_2$ grains. There are also some particles, such as particle 3, which are surrounded by three $Ce_{0.5}Zr_{0.5}O_2$ grains. Note that the Pd particles in figure 2(a) show different contrast, due to different crystallographic orientations with respect to the incident electron beam. Although about 15% of the Pd in the catalyst was not encapsulated after aging at 1150 °C, there were no PdO particles observed by TEM. This merely reflects the fact that these observations were confined to regions within the densified ceria–zirconia matrix, whereas the PdO particles would be located on external surfaces of the matrix.

It should also be noted that the apparent diameter of the particles is not exactly the same as the actual size of the particles. The particles are three-dimensional (3D) objects distributed in space. During the TEM specimen preparation, the 3D particles were sliced into disks. If a disk cuts through a particle via the center of the particle, the diameter of the observed particle (disk) is equal to the real diameter of the particle, otherwise, the apparent size of the particle is smaller. From a statistical point of view, the measured size distribution from the TEM images will thus be slightly biased toward small particles. Nevertheless, the particle size distribution measured by TEM is consistent with the results deduced from the XRD measurements which show that the average size of the particles is several tens of nanometers in diameter.

Unfortunately, it was not possible to confirm that the Pd particles imaged by TEM were under compressive stress as originally revealed by XRD, because the resolution of the microbeam electron diffraction measurements was insufficient to resolve the change in lattice constant. Further, slicing of the particles during sample preparation would almost certainly have allowed any residual stress to relax.

Particle growth is one of the most important contributing factors to thermal degradation of supported catalysts. Particle growth can occur via interparticle transport, with metal atoms diffusing either across the support surface or through the vapor phase. Another possible scenario involves particle migration, collision, and coalescence [5]. In our case, both the mixed-oxide support particles and the Pd metal particles undergo growth during thermal treatment. The initially high surface area (88 m^2/g) of the catalyst containing 2.25 wt% Pd on $Ce_{0.5}Zr_{0.5}O_2$ was reduced to less than 1 m^2/g after aging at 1150 °C. XRD and TGA measurements show that, after 1150 °C aging, large Pd particles have formed and become encapsulated by the cerium–zirconium mixed oxide under a distribution of stress states. Precursors to metal particle encapsulation have been observed in other catalyst systems. For example, in a TEM study, it was observed that Pt particles on silica become partially enveloped when annealed at 1200 and 1375 K [6]. As the driving force toward encapsulation, a reduction in surface free energy of the Pt/SiO_2 system was invoked. In systems containing metal particles on reducible oxides, such as Pt/TiO_2 or Ni/TiO_2, high-temperature reduction leads, according to a widely accepted interpretation of the strong metal–support interaction (SMSI) effect, to migration of TiO_x species onto the surface of the metal particles [7]. However, this effect is reversible and indicative of a decoration of the metal particles by oxide material rather than the deep, irreversible encapsulation observed here. Nevertheless, such SMSI processes (also reported for ceria) could be the starting point for the encapsulation which occurs at the high temperatures of this study.

Although the microstructure and chemical composition of the encapsulated Pd particles have been studied, the nature of the particle–matrix interface is not yet clear. Knowledge of the atomistic structure and atomic bonding at the interfaces formed between the ceria–zirconia matrix and the Pd particles is important in order to understand the underlying aging mechanism of the catalyst. Moreover, a detailed study of the catalysts at various stages during the aging process will also be critical for understanding the aging mechanism.

5. Conclusions

Spherical Pd particles with diameters ranging from 30 to 80 nm were observed by means of TEM in a Pd/ceria–zirconia catalyst after aging at 1150 °C. The particles were identified as pure Pd metal (rather than PdO) by means of EDS and microbeam electron diffraction. The Pd particles were found to be embedded, either within single grains or between several grains of ceria–zirconia. Elemental distribution maps derived from EDS imaging provided further confirmation of Pd particle encapsulation. These results are in complete accord with a previous study [2] which utilized only bulk methods, XRD and TGA, to deduce that Pd is encapsulated in this catalyst, but additionally provide a detailed picture of the actual microstructure. For future work, one interesting topic would be to study the particle surface (actually, the interface between the particles and the matrix) using high-resolution transmission electron microscopy.

Acknowledgement

This work was supported by the College of Engineering, University of Michigan, Ann Arbor, Michigan.

References

[1] J.-P. Cuif, S. Deutsch, M. Marczi, H.-W. Jen, G.W. Graham, W. Chun and R.W. McCabe, Society of Automotive Engineers Paper No. 980668 (1998).
[2] G.W. Graham, H.-W. Jen, W. Chun and R.W. McCabe, Catal. Lett. 44 (1997) 185.
[3] A.W. Hull, Science 52 (1920) 227.
[4] G.R. Levi and C. Fontana, Gazz. Chim. Ital. 56 (1926) 388.
[5] P. Wynblatt, R.A. Dalla Betta and N.A. Gjostein, in: *The Physical Basis of Heterogeneous Catalysis*, eds. E. Drauglis and R.I. Jaffee (Plenum Press, New York, 1975) p. 501.
[6] P.R. Powell and S.E. Whittington, J. Catal. 81 (1983) 382.
[7] H. Haberlandt, in: *Theoretical Aspects of Heterogeneous Catalysis*, ed. J.B. Moffat (Van Nostrand Reinhold, New York, 1990) chapter 8, p. 311, and references therein.